

A high precision VIS/NIR dynamic goniometer-spectrometer

Gennady Vishnyakov^{1,2} , Alexander Yurin^{3,*} , Vladimir Minaev^{1,3} 
and Alexander Goloposov¹ 

¹ All-Russian Research Institute for Optical and Physical Measurements, Moscow, Russia

² Bauman Moscow State Technical University, Moscow, Russia

³ HSE University, Moscow, Russia

E-mail: ayurin@hse.ru

Received 13 March 2023, revised 31 May 2023

Accepted for publication 19 June 2023

Published 28 June 2023



Abstract

We present a method for measuring the refractive index (RI) and spectral characteristics of transparent triangular prisms based on the minimum deviation technique. The proposed method has been developed to automatically measure RI simultaneously for three different wavelengths to determine the spectral dependence of RI. A high precision dynamic goniometer with a He-Ne ring laser and continuously rotating autocollimation mirror was used to implement the proposed method. A set of reference prisms made of optical glass were experimentally studied and the measurement uncertainty budget was estimated. The obtained values of the expanded measurement uncertainty did not exceed 4.6×10^{-6} for near-infrared and 1.2×10^{-5} for visible wavelength ranges with a coverage factor $k = 2$ (95% level of confidence). It is shown that this method can be used for high-precision measurements of the RI and determine the spectral characteristics.

Keywords: refractive index, refractive index measurements, dispersion, minimum deviation method, dynamic goniometer, spectrometer

(Some figures may appear in colour only in the online journal)

1. Introduction

The refractive index (RI) is an important characteristic of a substance in any of three aggregate states—solid, liquid, and gaseous. The RI is a dimensionless value equal to the ratio of the light speed in a vacuum to the light speed in the substance under study.

The section of optics devoted to methods and means of measuring the RI is called refractometry, and devices for measuring the RI are called refractometers [1]. The basis of these instruments is the phenomenon of refraction, which consists in changing the direction of the propagation of an electromagnetic wave (or light) at the interface between two

substances. This change of direction obeys the law of light refraction, discovered in 1621 by the Dutch scientist Snellius (1580–1626) [2].

Accurate and reliable refractometric measurements are necessary in the optical industry to increase the resolution of lenses and other optical devices [3]. Refractometers are used in the chemical industry to control the composition of substances [4], in the food industry for quality control of sugar, juices, alcoholic beverages, fats, oils, etc [5]. Pharmacological factories, medical institutions and pharmacies also widely use refractometers to analyze the composition and quality control of medicines [6].

Currently, there is a wide variety of refractometers. The study of the spectral dependence of the RI is needed to determine the dispersion characteristics of various substances, primarily optical glasses. Dispersion characteristics of optical

* Author to whom any correspondence should be addressed.

glasses are necessary for the calculation of precision optics with minimal chromatic aberrations [7]. In the production of glass for the optical industry, it is necessary to measure the principal dispersion, dispersion coefficients, and Abbe number of optical glasses [8], which require measuring the spectral dependence of the RI. Therefore, the new measuring instruments have appeared—spectral refractometers, for example, ATR-L Multiwavelength Spectroscopic Refractometer by *Schmidt&Haensch* (Germany), Abbemat MW by *Anton-Paar* (Austria), Abbe portable IRF—479A, IRF—479B by *JSC Shvabe—Technological Laboratory* (Russia).

The extension of the wavelength range at which the RI is measured from visible (VIS) to the near infrared (NIR) range up to 1550 nm is because it is necessary to determine the RI of optical materials (quartz, silicon, germanium, etc.), which are used in the manufacture of optical glass fibers, in the development of infrared optics for thermal imagers, night vision devices, etc. This article is devoted to the description and study of a goniometer-spectrometer based on a dynamic goniometer, which allows simultaneous measurements of the RI at several fixed wavelengths of radiation to reduce the time spent on determining the dispersion characteristics of the sample.

2. Measurement methods

RI measurement method is based on the refraction of light on passage through the boundary between two different substances. Goniometric methods based on measuring the angles of light deviation passing through the sample have become widespread due to their versatility, high accuracy, and ease of measurement. As samples, triangular prisms made of the material under study or filled with the substance under study are most often used, i.e. these methods can be applied to both solids and liquids. To measure the angles of the light deviation, special instruments are usually used—goniometers [9].

Various prism methods are often employed for precision RI measurements: autocollimation [10], minimum deviation [11], constant deviation, and grazing incidence (critical angle) [12]. We used the most popular minimum deviation method because it enables to attain the highest measurement accuracy [13]. Another important advantage is that the measurements can be automated completely. The essence of this method is to find such a position of the prism at which the minimum change in the direction of the incident beam is achieved.

2.1. Minimum deviation method

The method of measuring the RI used in a goniometer-spectrometer is based on measuring the angle of the minimum deviation of light when passing through an optically transparent triangular prism [14]. With an increase of the angle of incidence on the prism φ , the angle of deviation of the beam ϵ decreases, reaching a certain minimum—the angle of minimum deviation ϵ_{\min} , and then increases again, and the value of ϵ_{\min} mostly depends on the prism angle, RI and light

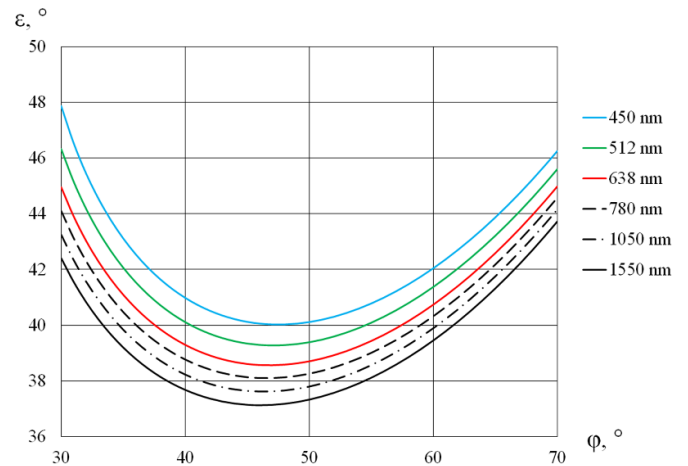


Figure 1. Dependence of the beam deviation angle on the angle of incidence at different wavelengths for a light flint prism with angle of 55°.

wavelength due to the dispersion characteristics of the prism material (figure 1).

By measuring the angle of the minimum deviation ϵ_{\min} , it is possible to calculate the relative RI of the prism material $n(\lambda, t)$ by the Fresnel formula [11]:

$$n(\lambda, t_{\text{prism}}) = \sin[(\alpha + \epsilon_{\min}(\lambda, t))/2] / \sin(\alpha/2), \quad (1)$$

where α is the prism angle, λ is the wavelength of light, t_{prism} is the temperature of the prism during measurements.

The RI of the material depends on the wavelength according to the Sellmeier equation [15]:

$$n^2(\lambda) = 1 + \sum_i \frac{A_i \lambda^2}{\lambda^2 - B_i}, \quad (2)$$

where A_i, B_i are experimentally determined Sellmeier coefficients of material.

The absolute RI of the prism material n_{abs} at the wavelength λ and its temperature t_{prism} is calculated by the formula [2]:

$$n_{\text{abs}}(\lambda) = n(\lambda, t_{\text{prism}}) n_{\text{air}}(t_{\text{air}}, p, f, \lambda), \quad (3)$$

where n_{air} is the RI of air, t_{air} is the air temperature, p —atmospheric pressure, f —partial pressure of water vapor.

The RI of air is calculated by the Edlen formula [16]. If the measurement conditions are differ from normal [17], then it is also necessary to introduce an amendment according to the following formula [18]:

$$n_{\text{abs}}(\lambda) = n(\lambda, t_{\text{prism}}) n_{\text{air}}(t_{\text{air}}, p, f) - \beta_{\text{abs}}(t - 20^\circ), \quad (4)$$

where β_{abs} is the prism material RI temperature coefficient.

The thermo-optical characteristics of optical glasses, including the RI temperature coefficient β_{abs} , can be found in the documents of companies producing that glass.

Thus, the final equation for measuring the RI of the prism material reduced to the normal conditions ($t = 20\text{ }^\circ\text{C}$; $p = 101.325\text{ kPa}$; $f = 1.33\text{ kPa}$) is as follows [18]:

$$n_{\text{abs}}(\lambda) = [n(\lambda, t_{\text{prism}})n_{\text{air}}(t_{\text{air}}, p, f, \lambda) - \beta_{\text{abs}}(t - 20^\circ)]/n_{\text{air0}}(\lambda), \quad (5)$$

where $n_{\text{air0}}(\lambda)$ is the RI of air under normal conditions.

3. Measurement requirements

3.1. Angles measurements requirements

Estimates show that to measure a RI with an error of $\pm 1 \times 10^{-6}$ requires primarily the measurement of prism angles and deviation angle at the level of tenths of an angular second [13].

Our high precision goniometer-spectrometer is based on a dynamic goniometer with a He-Ne ring laser or encoder [19], which provides the necessary accuracy characteristics of angle measurements with root mean square (RMS) better than $\pm 0.03''$ and standard uncertainty of $0.12''$.

The difference from an ordinary goniometer is that all the measurements with a dynamic goniometer are made under dynamic conditions with the autocollimation mirror rotating continuously. Our novel method has been developed to automatically determine ϵ_{min} simultaneously for several different wavelengths. The essence of our method is that we first perform a series of automatic measurements of deviation angle ϵ with various angular positions of the prism and then calculate ϵ_{min} for each wavelength.

3.2. Sample quality

The following are the main error sources when measuring a RI: error of measuring angles with the goniometer and errors of manufacture of the samples (prisms), due to prism working faces deviation from perpendicularity and planarity.

The pyramidal error consists of the working faces not being perpendicular to the base of the prism. As a result, a beam reflected from a face is deviated with respect to the optic axis of the collimator in the vertical direction, which leads to vignetting of the reflected beam and influences its intensity. The effect of this pyramidal error of the prism faces on the measurement accuracy increase as the RI increases [20]. In the standard equipment, the prism pyramidal error should not exceed $2''$. In that case it has no effect on the measurement accuracy with our method.

Nonplanar working faces leads to the angle of the prism being different from the nominal value. Consequently, the angle of deviation will also differ from the calculated value. Nonplanarity tests have shown that a deviation of $\lambda/10$ leads to the angle changing by tenths of an angular second, so deviation from planarity of the working faces of the prisms should not be greater than $\lambda/18$ [20].

3.3. Environmental conditions

The air and sample temperatures should be kept at constant values during the measurement, while the temperature of the prism and the surrounding parameters (air temperature, humidity, and atmospheric pressure) must be measured with high accuracy [13].

Using a further feature of such a goniometer-spectrometer is that we can perform measurements automatically without the presence of the operator in the measurement zone, i.e. the measurements may be made remotely. This also serves to resolve the problems of thermal stabilization for the measurement volume.

The necessary part of the measuring equipment should be placed in an insulated chamber, while the other units, which produce the main heat, are kept outside it.

The RI of air under normal conditions is $n_{\text{air0}}(\lambda)$, calculated by the Edlén formula for precisely specified meteorological parameters.

3.4. Light sources and detectors

To measure the RI on the different wavelengths we apply a different light sources of VIS/NIR ranges: 632.8 nm He-Ne laser (*Lumentum 1145P*) and laser diode modules (*LLC LasersCom LDI series*) with wavelengths of 450 nm, 512 nm, 780 nm, 1050 nm and 1550 nm. Three of these sources can be used simultaneously, the radiation of which is combined into a common beam using fiber-optic couplers. Laser diodes are selected in such a way that it is possible to obtain required angular resolution when measuring the value of the $\epsilon_{\text{min}}(\lambda)$ for neighboring wavelengths in a given spectral range and to determine the six coefficients of Sellmeier equation (2). The difference in the value of $\epsilon_{\text{min}}(\lambda)$ for the used wavelengths is tenths of a degree, which corresponds to a delay between successive signals at the radiation detector in units of milliseconds at a platform rotation speed of about 40 rpm.

We used *Hamamatsu G10899-03K InGaAs VIS/NIR photodiode* for detecting the light sources radiation.

4. Dynamic goniometer

To measure the desired $\epsilon_{\text{min}}(\lambda)$, a dynamic goniometer was used as a basic part of the goniometer-spectrometer (figure 2), measurements on which are performed with continuous rotation of the console 3 with a two-sided autocollimation mirror 2 fixed on it around the object stage 4. To determine the angle of the console rotation, a He-Ne ring laser was used [19], creating an angular scale.

To determine the angle of the beam deviation in a dynamic goniometer a two-sided mirror 2 was used, mounted on the edge of the rotating console 3 in a position where the normal to the mirror is perpendicular to the axis of rotation [18]. The investigated prism 5 is placed on a rotary object stage 4 in such a way that the radiation beam 8 falls on the input working face at a certain angle φ . Object stage 4 is not mechanically

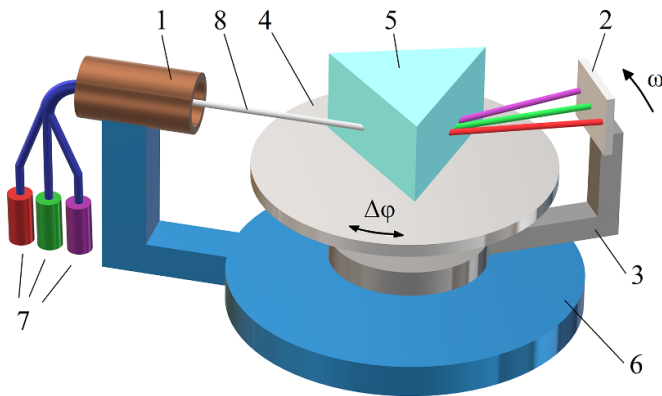


Figure 2. A goniometer-spectrometer based on a dynamic goniometer: 1—zero indicator; 2—two-sided mirror; 3—rotating console; 4—rotary object stage; 5—triangular prism; 6—fixed base; 7—laser diode modules; 8—radiation beam.

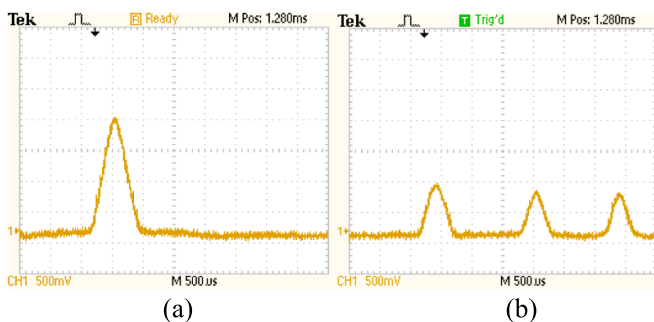


Figure 3. The oscillograms of photodetector signals obtained for 632.8 nm, 512 nm and 450 nm sources combined into a common beam: (a)—signal from the outer side of the autocollimation mirror; (b)—signal from the inner side of the autocollimation mirror.

connected to the rotating console 3 of the goniometer, and during the measurements the prism is stationary.

To bind to reflective surfaces, the goniometer uses a zero indicator 1, which produces pulses at those moments in time when the outgoing radiation beam falls normally to the surface of the two-sided autocollimation mirror. When the two-sided mirror rotates, the image of the input slit aperture of the autocollimator moves in the plane of the analyzing (output) slit. Therefore, the intensity of the light passing through the analyzing slit will be proportional to the area of overlap. If the width of these slits is the same, then the signal of light detector will have a shape close to a triangle, with a clearly marked maximum.

The first signal from the zero indicator, which sets the beginning of the angular measurements, occur when the beam is reflected from the outer surface of the two-sided mirror (figure 3(a)). The following signal, which sets the angle of deviation of the refracted beam with respect to the incident beam, occurs when reflected from the inner surface of the mirror [18]. Since the radiation beam is formed simultaneously by several laser modules 7, for one complete rotation of the

console with a two-sided mirror a series of sequential signals containing information about the deviation angles for each wavelength are received on the radiation detector because of prism material dispersion (figure 3(b)).

To find the $\epsilon_{\min}(\lambda)$ in automatic mode, a series of measurements is carried out for different angular positions of the prism relative to the incidence beam (i.e. for different angles of incidence φ_i , $i = 0, 1, 2, \dots, K$, where K is the total number of measurements), which are obtained by rotating object stage 4 at a certain fixed angle $\Delta\varphi$ using a stepper motor. The obtained dependences for each wavelength are approximated by a polynomial of the second degree and the corresponding value $\epsilon_{\min}(\lambda)$ is calculated. The results of numerical simulation showed that the interpolation error of calculating $\epsilon_{\min}(\lambda)$ does not exceed $\pm 0.03''$.

5. System description

5.1. Hardware

To perform the RI determination, our measuring system includes the following equipment (figure 4):

1. autocollimation zero indicator with photodetector;
2. a radiation source of the wavelength range from 450 nm to 1550 nm consists of five laser modules and He-Ne laser with a combined fiber optic output;
3. rotating console with autocollimation mirror and He-Ne ring laser;
4. rotary object stage with stepper motor;
5. electronic unit for data acquisition and stepper motor control;
6. multi-channel digital thermometer CA 320 with separate temperature sensors;
7. power supplies for laser modules and ring laser;
8. IVA-6 Thermohygrometer for air parameters control;
9. a system for collecting and processing measured data based on a personal computer (PC) with the original RefractiveIndexMeter software;
10. a climatic chamber with feedback thermal stabilization.

The main measuring equipment is located within a special chamber of volume 18 m^3 . The walls, floor, and ceiling of the chamber are made of special thermal insulation panels faced by sheet metal to reduce the temperature gradients. The chamber has a thermally insulated door for access and a window for visual monitoring. It is equipped with systems for humidifying and cleaning the air, and also with the thermohygrometer.

The basis of the goniometer-spectrometer is the dynamic goniometer DG-03L, developed by the St. Petersburg State Electrotechnical University (LETI), which provides a standard error of angular measurements less than $\pm 0.03''$, a systematic error not more than $\pm 0.2''$ and standard uncertainty of $0.12''$. In this goniometer, the zero indicator is made in the form of a photoelectric autocollimator, which forms and directs a flat beam of light, and then generates an electrical signal at the

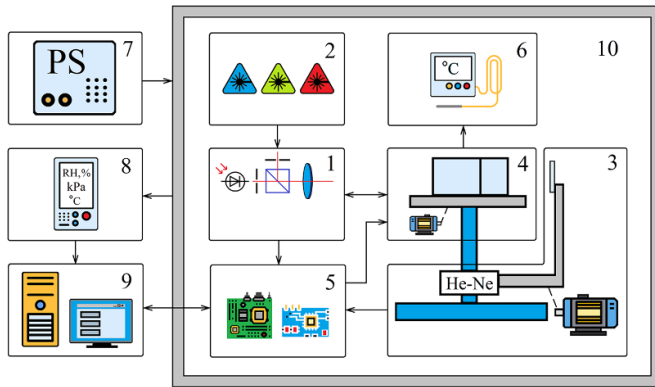


Figure 4. The schematic diagram of the measuring system: 1—zero indicator; 2—radiation source; 3—rotating console; 4—rotary object stage; 5—electronic unit; 6—thermometer; 7—power supplies; 8—thermohygrometer; 9—PC; 10—climatic chamber.

moments when the light beam reflected back. The radiation of light sources enters zero indicator via an optical fiber coupler.

The received signals enters the electronic unit, where they are digitized using a 12-bit analog-to-digital converter with 100 MHz sampling rate to determine the maximum. This unit also receives signals from the goniometer ring laser, using which the measured angles are calculated using RefractiveIndexMeter software.

The multichannel digital thermometer CA 320 is used to measure the temperature of the prism necessary to calculate the amendment in formula (4), and thermohygrometer IVA-6 measures the parameters of atmospheric air to calculate n_{air} according to the Edlen formula.

A PC with the RefractiveIndexMeter software calculates the angle of minimum deviation and the desired RI of the prism material, and also controls a rotary object stage.

Constant temperature within the chamber is maintained by a precision air conditioning system: a split system of inverter type. It provides temperatures of the air constant to $20.0\text{ }^{\circ}\text{C} \pm 0.1\text{ }^{\circ}\text{C}$ in the internal volume with active thermal stabilization. This system is disconnected during the measurements, which last several minutes.

To reduce the temperature gradients, the climatic chamber is located in a room also equipped with an air-conditioning system that maintains a temperature of $20\text{ }^{\circ}\text{C} \pm 1\text{ }^{\circ}\text{C}$.

The measurements are completely automated. The operator remains outside the chamber during the measurements. Main heat-producing units and measuring equipment (like power supply sources and PC) are placed outside the chamber.

For precision measurements, the optical equipment is mounted on an antivibration table, which provides reliable protection against the vibration. Therefore, our goniometer-spectrometer can be located in any building without special requirements for vibrational protection.

The chamber is equipped with a multichannel digital thermometer for measuring the temperatures of the prism and the air within the chamber. The limit to the permissible error in the thermometer measurements is $\pm 0.01\text{ }^{\circ}\text{C}$. The temperature

measurement system includes three separate detectors, two of which are placed inside the measurement volume and one contact detector is placed on the sample prism. The temperature data from all three detectors displayed on the PC's screen.

The data-acquisition and processing system consists of a PC equipped with analog-digital converter, interfaces for collecting the measurement data from the goniometer-spectrometer and the thermometers, and with software for processing the angular measurements and calculating the RI.

5.2. Software

All measurement operations carried out from PC using RefractiveIndexMeter original software. Software consists of two parts: software for angle measurements and software for RI calculation.

RefractiveIndexMeter calculates the desired RI of the prism material, and also provides control of the measurement process with the goniometer DG-03L, controls a rotary object stage driven by a stepper motor, calculates the angles of minimum deviation, collects meteorological conditions of the ambient air environment (temperature, humidity, atmospheric pressure) from the IVA-6 thermohygrometer.

A preliminary search for the position of the prism at which the deviation angle is close to its minimum value for the first received signal is carried out using stepper motor to rotate the object stage. After the preliminary search is completed, the process of accurately measuring the dependence of the angle of deviation from the angle of incidence is automatically started, followed by approximation of the obtained dependences by a 2nd degree polynomial at 9 points for each signal and the values of ϵ_{min} are calculated.

6. Experimental results

We used a set of reference prisms №01, №02 and №03 (Schott glass, Germany), which participated in international comparisons COOMET.PR-S3 [21] as samples. RI was measured simultaneously at VIS range wavelengths of 450 nm, 512 nm and 632.8 nm for each prism. Table 1 shows the obtained results of the RI measurements reduced to the normal conditions.

We repeated a similar experiment for the NIR range at wavelengths of 780 nm, 1050 nm and 1550 nm simultaneously (table 2).

Every experiment took several minutes, because for accurate measurements, the console makes 20 full rotations for each of 12 angular positions of the prism near to reaching ϵ_{min} .

Using measurement results, it is possible to find the spectral dependence of the RI and to compute the Sellmeier dispersion formula coefficients using the Zemax software [22]. Using those coefficients, it is easy to calculate the RI at any wavelength according to the formula (2). So, we calculated the value of RI for Fraunhofer lines [23] F (H 486.13 nm), d (He 587.56 nm) and C (H 656.27 nm) to determine the main dispersion characteristics of the prism material. Table 3 shows

Table 1. RI measurements results for VIS range.

Prism №, glass type	λ , nm	RI value	RMS $\times 10^{-6}$
№01, N-BAF 10	450	1.685 625	0.2
	512	1.677 075	0.2
	632.8	1.667 260	0.1
№02, N-BK 7	450	1.525 547	0.2
	512	1.520 904	0.2
	632.8	1.515 362	0.1
№ 03, SF-1	450	1.744 323	0.3
	512	1.728 999	0.2
	632.8	1.712 381	0.1

Table 2. RI measurements results for NIR range.

Prism №, glass type	λ , nm	RI value	RMS $\times 10^{-6}$
№01, N-BAF 10	780	1.660 948	0.4
	1050	1.655 282	0.6
	1550	1.650 642	0.8
№02, N-BK 7	780	1.511 507	0.7
	1050	1.507 188	0.5
	1550	1.501 979	0.6
№ 03, SF-1	780	1.702 148	0.5
	1050	1.693 230	0.5
	1550	1.686 052	0.7

Table 3. Dispersion characteristics calculation results.

Prism №, glass type	Abbe number $V_D = \frac{n_d - 1}{n_F - n_C}$	Principal dispersion $n_F - n_C$
№01, N-BAF 10	46.9876	0.014 263
№02, N-BK 7	64.1820	0.008 056
№ 03, SF-1	29.5188	0.024 300

the Abbe number and principal dispersion [24] calculation results.

7. Accuracy analysis

Since we used laser diodes with a sufficiently wide spectral characteristic $L(\lambda)$ (figure 5) as radiation sources, their influence on the angle measurements was investigated. So, we performed a simulation of the signal formation process on the detector after the radiation passes through the prism to determine the effect of the spectral characteristic of the source on the results of measuring the minimum deviation angle.

The signal formation occurs due to the rotation of the mirror around the prism, where the useful signal is formed at the moment of reflection of the refracted radiation in the opposite direction. In this case, the image of the input slit of the autocollimation zero indicator moves in the plane of the output slit, behind which there is a radiation detector. Thus, the resulting electric signal of detector $U(t)$ is a convolution of the

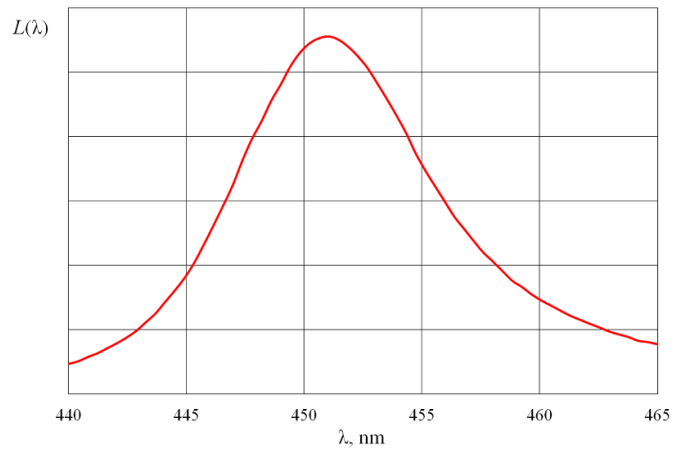


Figure 5. Typical spectral characteristic of a laser diode obtained using a Hamamatsu C10083CA spectrometer.

illumination distribution function of the image $E'(x)$ with the transmission function of the output slit $\tau(x)$, so

$$U(t) = \int_{-\infty}^{\infty} \tau(x)E'(x - \Delta xt)dx, \tag{6}$$

where Δxt is the offset at time moment t .

The maximum of the received signal is the reference data for measuring the ϵ_{\min} .

For simulation, the rotation frequency of the mirror of 40 rpm was set, and the illumination time of the detector $T_{il} = 0.01$ s. The known data are the normalized spectral characteristic of the radiation source $L(\lambda)$ and the spectral angle of minimum deviation $\epsilon_{\min}(\lambda)$ for a given prism.

For the convenience of calculations, we converted the dependence of the signal on time to the dependence of the signal on the angle of rotation of the mirror ϵ . The rotation period of the mirror T is about 1.5 s. According to the specified illumination time, we determine the angle of rotation of the mirror $\Delta\epsilon$ corresponding to the movement of the slit image by its own width as

$$\Delta\epsilon = 2\pi T_{il}/T. \tag{7}$$

Considering the width of the image of the input slit equal to the width of the output slit at any angle of rotation of the mirror, we will set the spectral distribution of illumination of the input slit by the expression

$$E'(\epsilon, \lambda) = \begin{cases} L(\lambda), & \epsilon_{\min}(\lambda) - \Delta\epsilon/2 < \epsilon < \epsilon_{\min}(\lambda) + \Delta\epsilon/2 \\ 0, & \epsilon_{\min}(\lambda) - \Delta\epsilon/2 > \epsilon; \epsilon_{\min}(\lambda) + \Delta\epsilon/2 < \epsilon \end{cases} \tag{8}$$

The polychromatic illumination will be determined by the expression

$$E'(\epsilon) = \int_{\lambda_1}^{\lambda_2} E'(\epsilon, \lambda)d\lambda, \tag{9}$$

where $\lambda_1 \div \lambda_2$ is the spectral range under consideration.

Table 4. The uncertainty budget of RI measurements for NIR wavelengths range.

Uncertainty source	Standard measurement uncertainty	Uncertainty contribution		
		Nº01, N-BAF 10	Nº02, N-BK 7	Nº03, N-SF1
Repeatability of RI measurements	1.0×10^{-6}	1.0×10^{-6}	1.0×10^{-6}	1.0×10^{-6}
Flatness of prism surfaces, radian	5.6×10^{-7}	3.1×10^{-7}	4.4×10^{-7}	4.1×10^{-7}
Prism angle α , radian	1.1×10^{-6}	9.7×10^{-7}	7.5×10^{-7}	1.1×10^{-6}
Angle measurements, radian	1.4×10^{-6}	7.8×10^{-7}	1.1×10^{-6}	1.0×10^{-6}
Angle of minimum deviation interpolation, radian	8.4×10^{-8}	4.7×10^{-8}	6.5×10^{-8}	6.2×10^{-8}
Wavelength λ , nm	0.6×10^{-1}	8.9×10^{-7}	7.7×10^{-7}	1.4×10^{-6}
Prism temperature t_{prism} , °C	5.8×10^{-3}	1.4×10^{-8}	6.3×10^{-9}	2.2×10^{-8}
RI of air, n_{air}	2.3×10^{-7}	3.8×10^{-7}	3.5×10^{-7}	3.9×10^{-7}
Total combined standard uncertainty		1.9×10^{-6}	2.0×10^{-6}	2.3×10^{-6}
Expanded uncertainty U_p ($k = 2$)		3.8×10^{-6}	4.0×10^{-6}	4.6×10^{-6}

The transmission of the output slit, depending on the angle of rotation of the mirror ϵ , will be defined as the projection of the input slit at a wavelength λ_{max} corresponding to the maximum of the spectral characteristic of the source:

$$\tau(\epsilon) = \begin{cases} 1, & \epsilon_{\min}(\lambda) - \Delta\epsilon/2 < \epsilon < \epsilon_{\min}(\lambda) + \Delta\epsilon/2 \\ 0, & \epsilon_{\min}(\lambda) - \Delta\epsilon/2 > \epsilon; \epsilon_{\min}(\lambda) + \Delta\epsilon/2 < \epsilon \end{cases} \quad (10)$$

Thus, the resulting signal, depending on the angle of rotation of the mirror ϵ , will be determined by convolution

$$U(\epsilon) = \int_0^{2\pi} \tau(\epsilon)E'(\epsilon - \Delta\epsilon)d\epsilon. \quad (11)$$

According to the described process of signal generation, a simulation was carried out. As a result, signals from an ideal monochromatic source and taking into account the spectral characteristics of the source were compared. The offset of the maximum of the detected signal for the used laser diodes did not exceed 0.2". We have added this value to the angle measurement errors.

The uncertainty budget was also evaluated (table 4). From experimental studies it was obtained that the standard deviation (RMS) of the RI measurements results in the entire wavelength range from 405 nm to 1550 nm does not exceed 1×10^{-6} , so the standard uncertainty $u_A(n)$ by type A will also be equal to the same value.

Based on the measurement equation (5), uncertainties of the following values contribute to the extended uncertainty of the RI measurement (standard uncertainties $u_B(n)$ by type B):

Table 5. Uncertainty budget of Abbe number and principal dispersion calculation result.

Prism Nº	Abbe number total combined standard uncertainty	Principal dispersion total combined standard uncertainty
Nº01	1.6×10^{-2}	4.9×10^{-6}
Nº02	2.3×10^{-2}	3.0×10^{-6}
Nº 03	1.0×10^{-2}	8.6×10^{-6}

- the flatness of prism surfaces;
- the prism angle α ;
- the deviation angle measurements;
- the minimum deviation angle interpolation;
- the wavelength λ ;
- the temperature of the prism t_{prism} ;
- the RI of air $n_{\text{air}}(t_{\text{air}}, p, f)$.

Type B measurement uncertainties were obtained using rectangular probability distribution of errors.

To calculate the uncertainty budget, sensitivity coefficients were determined by differentiating the expression (5). The numerical values of the sensitivity coefficients are dependent on the wavelength, so, for further estimates, these coefficients were calculated for a central wavelength of VIS/NIR ranges.

The obtained values of the expanded measurement uncertainty U_p of prisms Nº01, Nº02 and Nº03 for VIS wavelength range are 7.9×10^{-6} , 1.0×10^{-5} and 1.2×10^{-5} respectively with a coverage factor $k = 2$ (95% level of confidence).

An uncertainty budgets for the Abbe number and for the principal dispersion were evaluated too (table 5).

8. Conclusion

The method for measuring RI proposed in this article can be used to study triangular prisms made of optically transparent materials or liquid optically transparent substances filling a hollow triangular prism. The use of high precision dynamic goniometer with different radiation sources and coupled fiber-optic output makes possible the automated simultaneous measurements of the RI at three fixed wavelengths to reduce the time spent on determining the dispersion characteristics of the sample.

The proposed method was implemented using the State Primary Standard of the Refractive Index Unit GET 138-2021 of the All-Russian Research Institute for Optical and Physical Measurements. GET 138-2021 intended for storing, reproducing, and transmitting the unit size of RI of solid and liquid substances [25].

ORCID iDs

Gennady Vishnyakov  <https://orcid.org/0000-0003-0237-4738>

Alexander Yurin  <https://orcid.org/0000-0002-6401-5530>

Vladimir Minaev  <https://orcid.org/0000-0002-4356-301X>

Alexander Goloposov  <https://orcid.org/0000-0002-1223-204X>

References

- [1] Werner A 1968 Methods in high precision refractometry of optical glasses *Appl. Opt.* **7** 837
- [2] Born M and Wolf E 2013 *Principles of Optics: Electromagnetic Theory of Propagation, Interference and Diffraction of Light* (Amsterdam: Elsevier)
- [3] Lee C, Choi H, Jin J and Cha M 2016 Measurement of refractive index dispersion of a fused silica plate using Fabry–Perot interference *Appl. Opt.* **55** 6285–91
- [4] Doudou B, Chiba I and Daoues H 2022 Optical and thermo-optical properties of polyvinyl alcohol/carbon nanotubes composites investigated by prism coupling technique *Opt. Mater.* **31** 112672
- [5] Shehadeh A, Evangelou A, Kechagia D, Tataridis P and Chatzilazarou A 2020 Effect of ethanol, glycerol, glucose/fructose and tartaric acid on the refractive index of model aqueous solutions and wine samples *Food Chem.* **329** 127085
- [6] Kuiper M, Van de Nes A, Nieuwland R, Varga Z and Van der Pol E 2021 Reliable measurements of extracellular vesicles by clinical flow cytometry *Am. J. Reprod. Immunol.* **85** e13350
- [7] Greysukh G, Ezhov E, Levin I, Kalashnikov A and Stepanov S 2012 *Comput. Opt.* **36** 395
- [8] Wray J and Neu J 1969 Refractive index of several glasses as a function of wavelength and temperature* *J. Opt. Soc. Am.* **59** 774–6
- [9] Vishnyakov G, Levin G, Ziouzev G, Liudomirski M, Pavlov P and Filatov Y 2002 *Proc. SPIE* **4900** 150
- [10] Cheng C 2014 Refractive index measurement by prism autocollimation *Am. J. Phys.* **82** 214
- [11] ISO 21395–1:2020 Optics and photonics—test method for refractive index of optical glasses—part 1: minimum deviation method
- [12] Tilton L *Prism Refractometry and Certain Goniometrical Requirements for Precision* 2018 (London: Forgotten Books)
- [13] Tentori D and Lerma J 1990 Refractometry by minimum deviation: accuracy analysis *Opt. Eng.* **29** 160
- [14] Astrua M and Pisani M 2009 Prism refractive index measurement at INRiM *Meas. Sci. Technol.* **20** 095305
- [15] Efimov A 2007 *Eur. J. Glass Sci. Technol. B* **48** 235
- [16] Edlen B 1966 The refractive index of air *Metrologia* **2** 71
- [17] Tilton L 1935 Standard conditions for precise prism refractometry *J. Res. Natl Bur. Stand.* **14** 393
- [18] Vishnyakov G, Levin G, Kornysheva S, Zyuzev G, Lyudomirskii M, Pavlov P and Filatov Y 2005 Measuring the refractive index on a goniometer in the dynamic regime *J. Opt. Technol.* **72** 929
- [19] Pavlov P, Filatov Y and Zhuravleva I 2021 Calibration of rotary encoders with different interfaces by means of a dynamic goniometer *Opt. Eng.* **60** 074105
- [20] Vishnyakov G and Kornysheva S 2012 The effect of the manufacturing quality of the optical components on the accuracy of the measurement of refractive index by the goniometer method *Meas. Tech.* **54** 1372
- [21] Vishnyakov G, Fricke A, Parkhomenko N, Hori Y and Pisani M 2016 Report on supplementary comparison COOMET.PR-S3: refractive index *Metrologia* **53** 02001
- [22] ZEMAX Optical Design Program User's guide 2009 (ZEMAX Development Corporation)
- [23] Smith W 2000 *Modern Optical Engineering. The Design of Optical Systems* 3rd edn (New York: The McGraw–Hill Companies, Inc.)
- [24] ISO 12123–2018 Optics and photonics—Specification of raw optical glass
- [25] Vishnyakov G, Minaev V and Bochkareva S 2022 GET 138-2021 State primary refractive index standard *Meas. Tech.* **65** 307–14